ELSEVIER
Surface Science xxx (2002) xxx–xxx
SURFACE SCIENCE
www.elsevier.com/locate/susc

# Fractalization of silicon islands at a coverage close to 0.5 monolayers

Zeev Olami [a], Yishay Manassen [b,*], N. Ramesh Rao [b], Rami Dana [b]

[a] Department of Chemical Physics, The Weizmann Institute of Science, Rehovot 76100, Israel
[b] Department of Physics and the Ilse Katz Center for Nanometer Scale Science and Technology, Ben Gurion University, P.O. Box 653, Be'er Sheva 84105, Israel

Received 23 January 2002; accepted for publication 8 August 2002

**Abstract**

Fractal islands are normally observed when the growth is a result of many random coalescence events of small islands or atoms with the growing cluster. In this paper, we show that fractalization can be observed also for growing islands at a coverage which is close to 0.5 monolayers. This was shown for a Si(1 1 1) surface covered by 0.53 monolayer of silicon. This fractalization is explained by the simple conservative Ising model, where the diffusion of a single atom is simulated by a single spin flip. In this model, fractal islands are observed over a finite scaling range where smaller islands have a dimension of 2 and larger ones are fractal. The fractal dimension and the scaling range are dependent on the fraction (equivalent to coverage) $p$ of spin up (or down). Both the dimension and range increase as $p$ approaches 0.5. We show that the growth of the clusters is in agreement with a classical $t^{0.33}$ law [Phys. Rev. B 34 (1986) 7845].


*Keywords:* Scanning tunneling microscopy; Growth; Monte Carlo simulations; Silicon; Dendritic and/or fractal surfaces

## 1. Introduction

The diffusion of atoms or clusters and their coalescence may sometimes give ramified islands with distinct fractal dimension. These ramified fractal islands were investigated many times with scanning probe microscopy on different surfaces [2–6]. This normally happens when the growth of the islands happens according to the scenario described by the diffusion limited aggregation (DLA) and related models. In the past the possibility of getting domains of fractal structure in systems where a dynamic phase separation of a mixture of two phases occurs (Ostwald ripening) was discussed. It was claimed that in the case where the two phases are comparable, the early stage morphology is fractal [7].

Ostwald ripening [8–10] is the non-equilibrium dynamics of a two phase system after a quench to a state in which it is no longer at equilibrium. The nucleation starts with a creation of small clusters and their on-going non-equilibrium dynamics is the issue which is under consideration. This is one of the classical problems in condensed matter physics. If the coarsening is dominated by atomic diffusion between islands the driving force to do-

* Corresponding author. Tel.: +972-7-6472-153; fax: +972-7-6472-904.
*E-mail address:* manassen@bgumail.bgu.ac.il (Y. Manassen).

0039-6028/02/$ - see front matter © 2002 Published by Elsevier Science B.V.
PII: S0039-6028(02)02270-7

main growth is the surface tension. The classical mean field theory of Lifshitz, Slyozov [11] and Wagner [12] (LSW) would hold. This theory assumes a small coverage (in two dimensions). For higher coverages one can observe correlations between the clusters [13]. Other possible models for coarsening are conservative surface models where coarsening occurs through the migration of atoms between neighboring sites. The simplest model of this type is the conservative Ising model (CIM). At higher coverages, the clusters are no longer compact. In this case, the shortest distance between the boundaries of different clusters, their minimal scale, is used to characterize their dynamics. It was argued by Huse [1] and confirmed in more extensive simulations that the minimal scale in such a process should be proportional to $t^{0.33}$ [19]. Renormalization group arguments lead to the same results [10,14]. In a later paper there was an initial attempt to simulate the scales of realistic clusters in the problem [15].

We are interested in the characteristics of larger islands. We have studied this point experimentally by looking at the morphological evolution of a surface covered by half a monolayer. In this case, the two phases that separate are atoms and vacancies. We have studied the problem theoretically by using the CIM to simulate coverages close to half a monolayer.

We find that silicon clusters at a coverage close to 0.5 monolayer are fractal with a well defined fractal dimension. In the experiment, the islands were fractal up to a system scale which is determined by the scan range of the STM. Although we could see a negligible number of larger islands at larger images, the resolution in this case did not permit any analysis.

We also find that clusters in the CIM case have a fractal dimension over a limited range, which seems to diverge at $p = 0.5$. There are two characteristic scales which define the behavior of the system at long times. These are the lower and upper scales of the fractal range. The upper scale, initially much smaller than the system size (lattice taken for the simulation), grows until it reaches this size. The ratio between the upper and the lower scale becomes a constant as a function of time. Clusters in the CIM case have a changing fractal dimension which is a function of the coverage $p$.

We find that at initial stages all the clusters do not show any fractality. At later stages, clusters with dimension of 2, appear at the smaller scaling range and at the larger scaling ranges the clusters are fractal over a limited fractal range. As the clusters grow in time the ratio between the upper and the lower scales in this range is constant. As $p$ is enlarged, the fractal dimension and the fractal range grow. This is an indication that as $p$ approaches 0.5 the fractal range grows to infinity. In addition we show that the dynamics of growth of these clusters is in agreement to the one observed by Huse.

In the first section we discuss the STM images of Si islands. The shape of these islands is not compact and they have a self-affine configuration. Such islands indicate a dynamics which is dominated by coalescence and were observed before in a coverage close to 0.5 [16]. We get that the islands are fractal over a limited scaling range. In the second section we discuss the CIM. In the last section we draw some general conclusions from these two observations.

## 2. STM of silicon fractal islands

A Si(1 1 1)7 × 7 surface with a coverage of silicon atoms close to a half was chosen in order to demonstrate this phenomenon. Our experiments were performed with a custom—made STM. The experiment begins by deposition of silicon from an electron gun evaporator on a clean Si(1 1 1)7 × 7 surface—at room temperature. The coverage was monitored by a quartz crystal monitor with an accuracy of approximately ±5%. After the deposition which created half a mono-layer of silicon on the Si(1 1 1)7 × 7, the surface was annealed for 5 min for 550 °C. This induces crystallization of the adsorbed layer and afterwards, starts the coarsening process. In previous studies [17,18] this was used for studying the low coverage (of voids) case.

STM images of this surface show that the surface is covered by ramified islands that were located very close to each other. Fig. 1 shows two typical STM images with fractal atomic islands

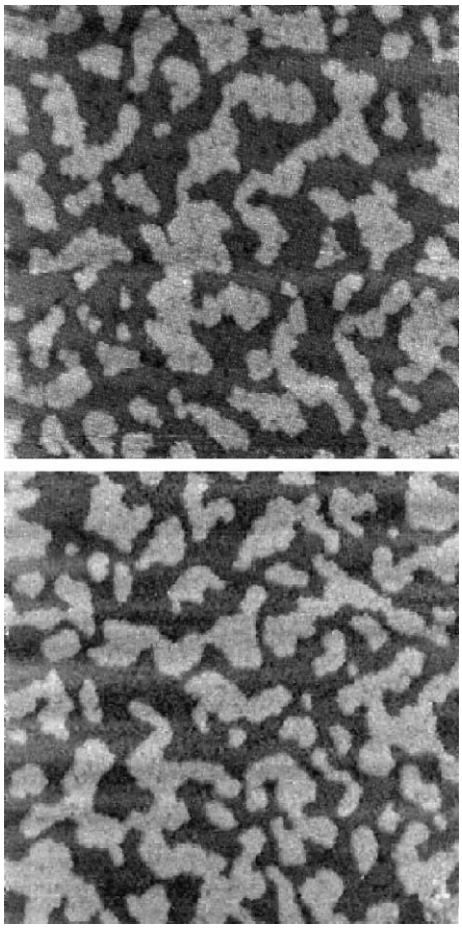

Fig. 1. Two STM images of a Si substrate after deposition of 0.53 monolayers of silicon and heating. The size of the STM images is $180 \times 180$ nm$^2$.

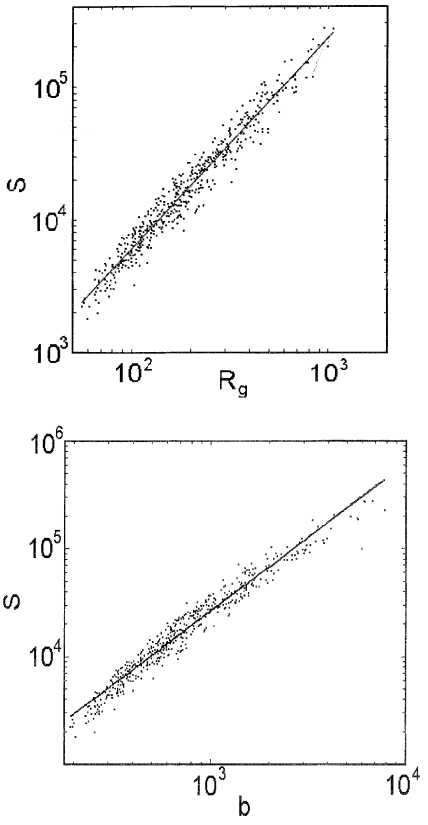


Fig. 2. The area of clusters observed in the experiment as a function of the radius of gyration of the cluster (top). Fitting the results to a power law we get $D = 1.58$. The area of the same clusters as a function of the their boundary (bottom). Here we get $D_b = 1.36$.

formed after a deposition of 0.53 monolayer. One can see a significant number of large clusters which are truncated by the boundary of the image.

We find that there is a continuous void background even when the coverage of voids is only 0.47. In order to analyze quantitatively the islands within this background one can calculate the radius of gyration $R_g$ of the clusters or the boundary length $b$. We find scaling of the area ($S$) with the radius of gyration $R_g$ and the boundary of the clusters $b$ of the type:

$$S = R_g^D \tag{1}$$

$$S = b^{D_b} \tag{2}$$

Note that these exponents are different from the well known Hausdorff dimension of the perimeter $A$ careful analysis of the shape of the islands was done to eliminate the area (defined as the number of pixels) of the clusters $S$, the radius of gyration of the clusters $R_g$, and the length of the boundary of the clusters $b$. In Fig. 2 we show log–log plots of $S$ as a function of $R_g$. 500 islands were analyzed to observe these plots. According to the fit to the power law, $D = 1.58 \pm 0.04$. We also found that $D_b = 1.36 \pm 0.04$ (defined at Eq. (2)). The limited range of the fractal dimension is a result of the finite size of the images. This suggests that fractal islands exist also beyond this size, and that the range of fractal dimension is larger. The islands are fractal over the whole scaling range although

we see that the smallest islands have a higher dimension. The reason for this will be explained later.

Another experiment was performed at a coverage of 0.76 (namely coverage of voids of 0.24) (Fig. 3). Fitting a power law to the experimental results gives an exponent of 1.56. However, a closer look at Fig. 3-center reveals that the smaller islands have a better fit to a power law of 2, while the larger islands, to a power law of 1.4. It seems that, at this coverage, the fractal dimension is smaller, that a larger number of (smaller) compact islands (with $D = 2$) exists, and that the range of island sizes in which the islands are fractal is smaller than in the previous case (Fig. 2).

## 3. Simulations on the CIM

A model that will explain these observations in a simple way, must take into account the following characteristics of the process: The motion of atoms is a simple diffusive motion, and when an atom migrates to a neighboring site, it can be viewed as an exchange process between an atom and a next nearest neighbour vacancy (when there are no next nearest neighbour vacancies the atom can not diffuse). Also, the growth process is driven by the interaction between atoms that make clusters of atoms more stable than isolated atoms. The simplest point of view that can be adopted is that the diffusion of an atom depends only on the local configuration. It was recognized long ago that the CIM is an appropriate description of this scenario [1].

The CIM is defined by two kinds of spins $s_i$(up/down) which interact through coupling: $H = \sum J s_i s_j$. When the model is conservative, spins switch places through the previous interaction. Like Huse we discuss the two dimensional case. The spins are our way of modeling atoms on a lattice. I.e. vacancies can be represented by the down spins while adatoms are represented by the up spins. We used a square lattice. This is different from the triangular structure of the Si(1 1 1) surface. Note that this is a somewhat naive representation of crystalline lattices since it is symmetric and does not contain more complicated interactions.

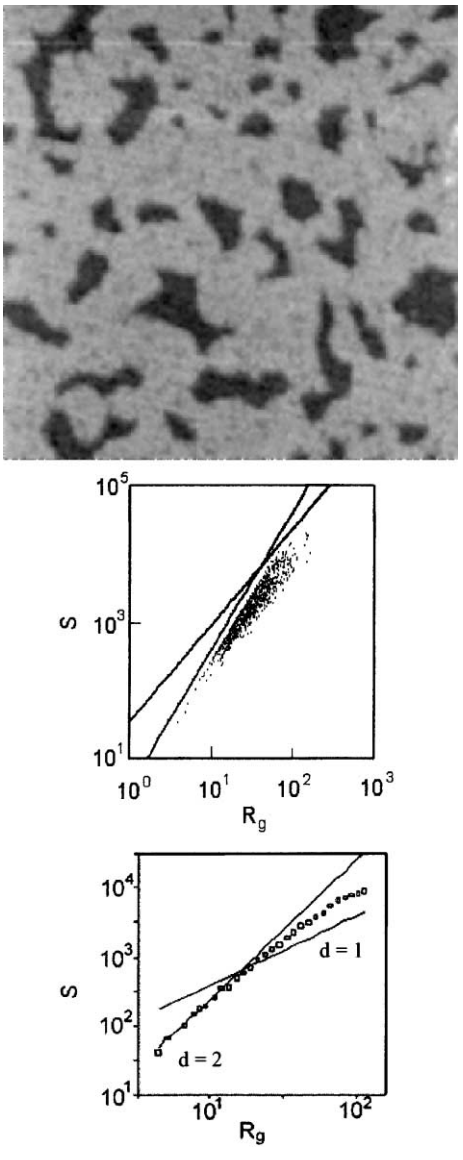


Fig. 3. Top: an STM image of a Si substrate after deposition of 0.76 monolayers of silicon and heating. The image is $180 \times 100$ nm$^2$. Center: the area of the cluster as a function of the radius of gyration or this coverage for 1000 islands. As a guide to the eye the curves $y = x^2$ and $y = x^{1.4}$ were added. Bottom: the points in the previous graph after averaging the points within the bin size. The curves $y = x^2$ and $y = x$ were added for clarity.

We performed Monte-Carlo simulations on the CIM with a Kawasaki dynamics where neighboring spins are exchanged according to their energy. The temperature is measured in units of the in-

teraction constant $J$. We performed a simple simulation of the exchange. We choose a temperature of $T = 0.6J$ for most of our simulations, but the results reported here are not dependent on the temperature. Our simulation times varied according to the coverage. For larger coverages we simulated till the clusters reached the scale of the system. This causes smaller running times in such coverages. We used periodic boundary conditions in all the simulations. We used lattices that consisted of up to $5000 \times 5000$ points. The cluster sizes are given in units of number of points. The number of steps in the simulation was up to 1 000 000.

We display two simulated lattices in Fig. 4 at $p = 0.25$ and 0.45. In the first case we observe clusters with a limited size range. Some of the clusters were formed by a merger of two clusters.

In the second case ($p = 0.45$) one observes elongated islands with a very large variation in the cluster scale and structure in the background of the voids. In the simulations although the islands had a ramified shape at early stages, they did not have a uniform and well defined fractal dimension at early stages as was proposed earlier [7].

In contrast at later stages we find that at the scaling ranges of the small islands the dimension is two, but at the scaling ranges of the larger islands a different dimension appears (Figs. 5 and 6). the fractal range increases as the coverage approaches to 0.5 This is largely due to the increase in the maximum island size.

In our simulations clusters are defined by the connectivities of the points on them. This always creates problems in smaller times but after the minimal scale grows to a significant range they become well defined. One can calculate the radius of gyration $R_g$ of the clusters or the boundary length $b$. We find scaling of the area of the clusters $S$ as a function of the radius of gyration $R_g$ and the boundary $b$ as was done for the experimental islands (Eqs. (1) and (2)).

Previous studies on similar systems [1,19] were largely focussed on the minimal scale of the structures. The main conclusion of these papers was that it grows according to the classical temporal power law $t^{0.33}$. In contrast, here one has to discuss the larger scale features of the structure.

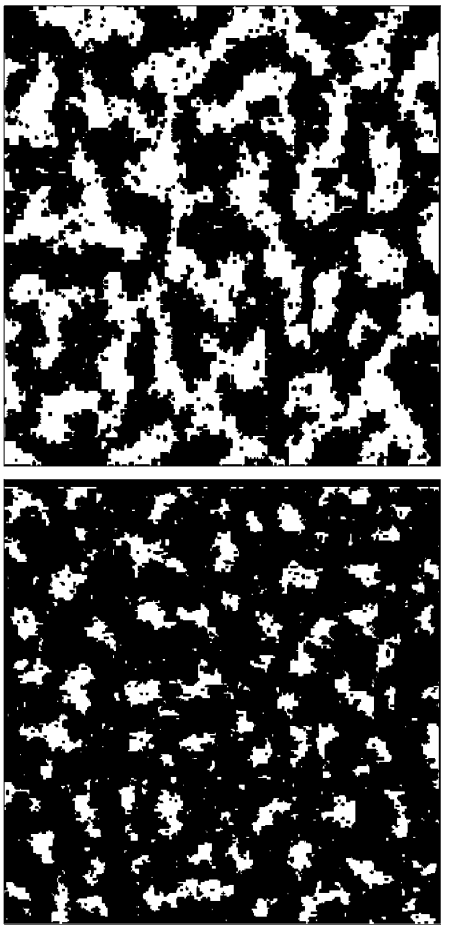

Fig. 4. Top: a lattice generated through a numerical simulation at $p = 0.45$. The total size of the simulation is $2000 \times 2000$ points, of which $250 \times 250$ lattice units are shown. Black is the void background. Later we calculate the fractal dimensionality of the islands. Bottom: a similar lattice generated through a numerical simulation at $p = 0.25$.

We present the scaling observed in the simulations for the coverages $p = 0.4$, 0.25 for different times. The first graph (Fig. 5) is constructed from a simulation of a lattice with a scale of 2000, while the second graph (Fig. 6) is from a lattice with a scale of 500.

One can clearly see that gradually a function which is composed of two regions is observed for the lower scaling ranges the dimension is two as can be seen in Figs. 5 and 6. For the upper scaling ranges it is $1.0 \pm 0.05$ for the 0.25 case while it is $1.40 \pm 0.05$ for the 0.4 case. This was calculated by

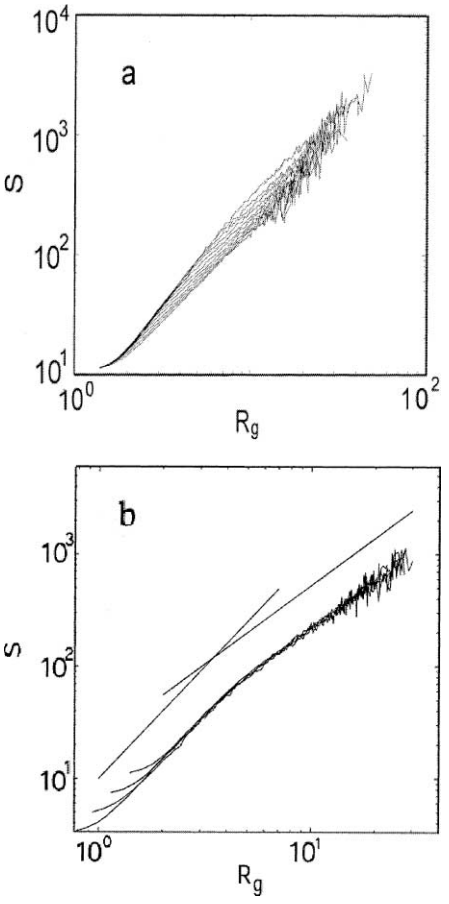


Fig. 5. (a) The area of the clusters ($S$) as a function of the radius of gyration ($R_g$) for $p = 0.4$ for different times ($2^j$, $j = 5$–19). (b) Right: a plot of the last four curves shown in Fig. 2a when they are rescaled (divided) by $t^{0.33}$ in the radial dimension and by $t^{0.66}$ in the area. Notice that these last curves overlap. Left: the curves $y = x^2$ and $y = x^{1.4}$ are added for clarity. Note the clear cut existence of two scaling regions.

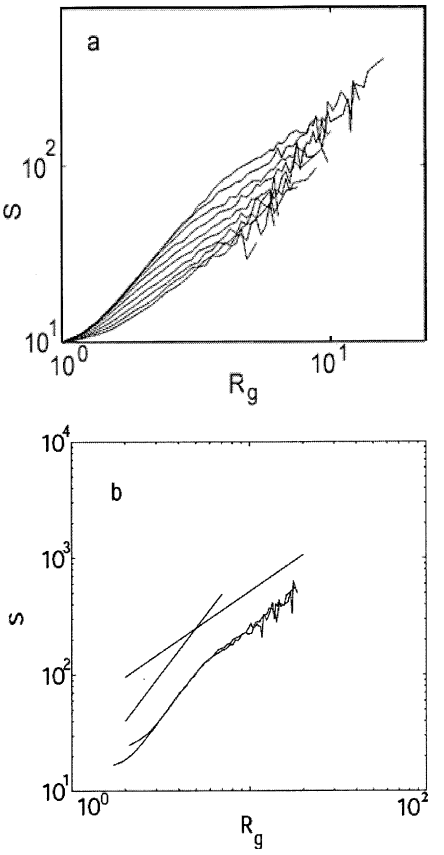


Fig. 6. (a) The area $S$ as a function of the radius of gyration $R_g$ for $p = 0.25$ at different times ($2^j$, $j = 5$–16). (b) Right: a plot of the last two curves in Fig. 5a when they are rescaled (divided) by $t^{0.29}$ in the radial dimension and $t^{0.58}$ in the area. Notice again, that curves overlap. Left: the curves $y = x^2$ and $y = x$ are added for clarity. It is possible, again, to identify two scaling regions.

fitting a line to the data in the log–log plot. The errors were estimated from the variance of this fit. An associated scaling by $t^{0.33}$ and $t^{0.66}$ of the late stage curves in Fig. 5a gives an overlap which is given in Fig. 5b. This overlap shows that both the smaller (compact) islands, as well as the cross over scale from compact to fractal islands grow according to the usual $t^{0.33}$ law.

The data in Fig. 6 were taken in shorter times than that of Fig. 5. It is well known that due to finite size effects, the dynamic exponent in shorter times is smaller than 0.33, and it reaches 0.33 only at very long time [1]. Indeed, we see that the exponent that is suitable here is 0.29 (Fig. 6b). Note, however, that an overlap is observed.

The results of the simulations indicate that the ratio between the largest fractal island and the smallest one (the upper scaling range in $R_g$) becomes time independent. The errors written in Table 1 were estimated from the variability of the fractal dimension and range in successive simulations.

A scan over other coverages shows that there is a continuous dependence of the fractal dimension and the scaling range in the cluster size on the

Table 1
The fractal exponents in the upper scaling range

| Coverage | Upper scaling range in $R_g$ | $D$ |
|---|---|---|
| 0.45 | $12.7 \pm 1$ | $1.5 \pm 0.05$ |
| 0.44 | $12.0 \pm 1$ | $1.5 \pm 0.05$ |
| 0.4 | $7.3 \pm 1$ | $1.4 \pm 0.05$ |
| 0.375 | $6.0 \pm 1$ | $1.2 \pm 0.05$ |
| 0.35 | $4.5 \pm 1$ | $1.2 \pm 0.05$ |
| 0.3 | $3.6 \pm 0.5$ | $1.0 \pm 0.05$ |
| 0.25 | $2.7 \pm 0.3$ | $1.0 \pm 0.05$ |

The scaling range for the upper exponent is given by the ratio between the upper cutoff and the lower one in the upper scaling range.

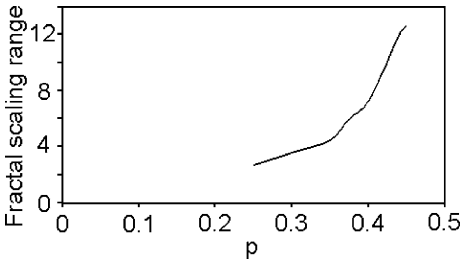


Fig. 7. The upper (fractal) dynamic range as a function of the coverage $p$. The divergence of the dynamic range as $p$ approaches 0.5 is clearly seen.

coverage $p$. This is summarized in Table 1 and Fig. 7. The fractal dimensions change from 1.5 to 1 at lower coverages, while the range (in which the clusters are fractal) drops to 2.7 for $p = 0.25$. The ranges in Table 1 were calculated from successive plots of the type of Figs. 5 and 6. The scales were estimated by a comparison between successive dynamical ranges in the long time limit. Because of this reason we do not observe significant cross-over behavior. The simulations are completely symmetric with respect to an interchange of voids and islands, so the results for $p > 0.5$ can always be constructed from those for $p < 0.5$ by taking $p' = 1 - p$.

The result of the simulation, that there will be a reduction of the fractal dimension and the fractal range in coverages much smaller (or larger) than 0.5 is supported, to some extent, by the experimental results that were presented in Fig. 3. It seems that, indeed, at this small coverage, the fractal dimension and range are smaller in coverages far from 0.5.

## 4. Discussion

With all the differences there is a basic similarity between the experimental results and the simulations. Despite its simplicity, the clusters observed in the CIM are fractal, as the silicon islands observed in the STM experiment.

To provide further insight to why these fractal islands are observed, one has to start from the low coverage limit: It is well known that for Lifshitz Slyozov growth in small coverages the fractal dimension is two. However, if $p$ grows the first phenomenon that will be observed is the effect of a merger of pairs of clusters. The smaller island will have an obvious dimension of 2 but few larger ones will have a fractal dimension As the coverage gets closer to 0.5, the clusters (islands) are restricted within a more and more complex labyrinth of the other type of spins (voids). Small clusters can still relax to a dimension of two without a collision. But larger ones will collide with the boundaries of other clusters in the labyrinth as a result of the relaxation process and will necessarily create larger clusters with a more complicated structure. This is a robust mechanism for the creation of larger (and more fractalized) clusters. The increase in the number of such collisions as $p$ grows, will widen the range of fractality by creating more fractal islands.

The diffusive relaxation of the clusters is responsible for the increase of the minimal scale in the structure as $t^{0.33}$ [1]. As was discussed above, at lower scales compact islands are observed (with unhindered relaxation), while at the larger scales the islands are fractal as shown in Figs. 2, 4, 5 and 7. Since the minimal scales grow as $t^{0.33}$ the cross over scale between $D = 2$ and $D < 2$ grows with the same temporal power law, as shown in Figs. 4 and 5.

Comparing the experimental results with the simulations reveals some contradiction between the fractal dimension which is observed by the experiment, and what is observed from the simulation. The fractal dimension of the silicon islands, is the same as the fractal dimension of the clusters with a coverage of 0.46 of islands in the CIM (not included in Table 1). In the CIM in this coverage, the infinite background is formed by voids which

are in a coverage of 0.53 and are in majority. In the experiment, the infinite background is also formed by voids, but they are in a coverage of 0.47 and in minority. Nevertheless, the fractal dimensions are similar in both cases. The reason for this shift is, most likely, the difference in tension between islands and voids. The curvature of islands and voids of the same size is opposite in sign, and this is expected to have a significant influence on the tension in the boundary and on the growth process. In the CIM, the curvature of the cluster is the same, whether it is an island or a void. This question is currently investigated.

Another difference between the experimental results and the simulations, is the appearance of a range of dimension of two in the lower scales—in the simulation. Nevertheless one can see bending of the scaling curves (Figs. 2 and 3) of the experimental islands at lower scales.

In this paper we showed that in the CIM the fractal dimension of clusters is observed over a finite range for growth in coverages which are smaller than $p = 0.46$. Our results show that the fractal range grows as the coverage is increased and they strongly indicate that there is a phase transition at $p = 0.5$ where the fractal range diverges. We present STM images on Silicon surfaces where the same phenomenon is observed. Current experimental and theoretical work is being dedicated to what happens when $p$ approaches closer to 0.5.

It is clear that the STM experiments described in this paper are just one example for the possibilities of studying many correlation and fractalization phenomena when atoms, detected by STM, are used as diffusing units on the surface at high coverage. Also, there are many questions of general interest that are connected to this experiment ranging from the electronic structure of confined electrons in such islands in systems that form two dimensional electron gas [20] to the possibility of investigating lateral tunneling between neighboring islands in such systems.

**Acknowledgements**

This work was supported by a grant from the Israel Science Foundation, founded by the Israeli Academy of Sciences and Humanities. Additional Support was given by grants from the German Israeli Binational Foundation for Research and Development (GIF) and from Intel.

**References**

[1] D.A. Huse, Phys. Rev. B 34 (1986) 7845.
[2] H. Roder, E. Hahn, H. Brune, J.P. Bucher, K. Kern, Nature 366 (1993) 141.
[3] R.Q. Hwang, J. Schröder, C. Günther, R.J. Behm, Phys. Rev. Lett. 67 (1991) 3279.
[4] Th. Michely, M. Hohage, M. Bott, G. Comsa, Phys. Rev. Lett. 70 (1993) 3943.
[5] Z. Zhang, X. Chen, M.G. Lagally, Phys. Rev. Lett. 73 (1994) 1829.
[6] T.-C. Chang, I.-S. Hwang, T.T. Tsong, Phys. Rev. Lett. 83 (1999) 1191.
[7] W. Klein, Phys. Rev. Lett. 65 (1990) 1462 and references therein.
[8] W. Ostwald, Z. Phys. Chem. (Munich) 34 (1900) 495.
[9] J.D. Gunton, M. San Miguel, P.S. Sanhi, in: C. Domb, J.L. Lebowitch (Eds.), Phase Transitions and Critical Phenomena, vol. 8, Academic Press, New York, 1983.
[10] A.J. Bray, Adv. Phys. 43 (1994) 357.
[11] I.M. Lifshitz, V. Slyozov, J. Phys. Chem. Solids 19 (1961) 35.
[12] C. Wagner, Z. Elektrochem 65 (1961) 581.
[13] O. Krichevsky, J. Stavans, Phys. Rev. Lett. 70 (1993) 1473; Phys. Rev. E 52 (1995) 1818.
[14] A.J. Bray, Phys. Rev. Lett. 62 (1989) 2841; Phys. Rev. B 41 (1990) 6724.
[15] T.B. Liverpool, Physica A 224 (1996) 589.
[16] M.S. Hoogeman, M.A.J. Klik, R. van Gaste, J.W.M. Frenken, J. Phys. Condens. Matter 11 (1999) 4349.
[17] E. Ter Ovanesyan, Y. Manassen, N. Ramesh Rao, Z. Olami, J. Vac. Sci. Technol. B 15 (1997) 1317.
[18] Y. Manassen, N. Ramesh Rao, I. Mukhopadhyay, E. Ter-Ovanesyan, Z. Olami, Phys. Rev. E 59 (1999) 2664.
[19] J.G. Amar, F. Sulivan, R.D. Mountain, Phys. Rev. B 37 (1988) 196.
[20] J. Li, W.-D. Schneider, R. Brendt, O.R. Bryant, S. Crampin, Phys. Rev. Lett. 81 (1998) 4464.